



**HAL**  
open science

## Genetic investigation of purine nucleotide imbalance in *Saccharomyces cerevisiae*

Christelle Saint-Marc, Johanna Ceschin, Benoît Pinson, Claire Almyre, Bertrand  
Daignan-Fornier

► **To cite this version:**

Christelle Saint-Marc, Johanna Ceschin, Benoît Pinson, Claire Almyre, Bertrand Daignan-Fornier. Genetic investigation of purine nucleotide imbalance in *Saccharomyces cerevisiae*. *Current Genetics*, 2020, 66 (6), pp.1163-1177. <10.1007/s00294-020-01101-y>. <hal-03379696>

**HAL Id: hal-03379696**

**<https://hal.science/hal-03379696v1>**

Submitted on 15 Oct 2021

**HAL** is a multi-disciplinary open access archive for the deposit and dissemination of scientific research documents, whether they are published or not. The documents may come from teaching and research institutions in France or abroad, or from public or private research centers.

L'archive ouverte pluridisciplinaire **HAL**, est destinée au dépôt et à la diffusion de documents scientifiques de niveau recherche, publiés ou non, émanant des établissements d'enseignement et de recherche français ou étrangers, des laboratoires publics ou privés.



HAL Authorization

[Click here to view linked References](#)

# Genetic investigation of purine nucleotide imbalance in *Saccharomyces cerevisiae*

Christelle Saint-Marc<sup>1,2,3</sup>, Johanna Ceschin<sup>1,2,3</sup>, Claire Almyre<sup>1,2</sup>, Benoît Pinson<sup>1,2</sup>, Bertrand Daignan-Fornier<sup>1,2,\*</sup>

<sup>1</sup> IBGC, Université de Bordeaux UMR 5095, Bordeaux, France;

<sup>2</sup> Centre National de la Recherche Scientifique IBGC UMR 5095, Bordeaux, France

<sup>3</sup> These authors contributed equally to the work

\*corresponding author

Christelle Saint-Marc<sup>1,2</sup> 0000-0001-9537-1848

Johanna Ceschin<sup>1,2</sup> 0000-0001-7771-531X

Bertrand Daignan-Fornier<sup>1,2,\*</sup> 0000-0003-2352-9700

Benoît Pinson<sup>1,2</sup> 0000-0003-2936-9058

## Keywords

Yeast metabolism, AMP deaminase, adenine deaminase, GTP, amino acid transport

## Declarations

### Funding

This work was supported by CNRS and Université de Bordeaux

### Conflicts of interest/Competing interests

The authors declare no conflict of interest

### Ethics approval

Not Applicable

### Consent to participate

Not Applicable

### Consent for publication

Not Applicable

### Availability of data and material

Not applicable

### Code availability

Not applicable

**Authors' contributions** Conceptualization: Daignan-Fornier; Methodology: Saint-Marc, Ceschin, Almyre, Pinson; Formal analysis and investigation: Saint-Marc, Ceschin, Almyre, Pinson; Writing - original draft preparation: Daignan-Fornier, Pinson; Writing - review and editing: Daignan-Fornier, Pinson; Funding acquisition: Daignan-Fornier; Supervision: Daignan-Fornier

## 38 Abstract

1  
2 39 Because metabolism is a complex balanced process involving multiple enzymes, understanding how  
3 40 organisms compensate for transient or permanent metabolic imbalance is a challenging task that can be  
4 41 more easily achieved in simpler unicellular organisms. The metabolic balance results from the  
5 42 combination of individual enzymatic properties, regulation of enzyme abundance, but also from the  
6 43 architecture of the metabolic network offering multiple interconversion alternatives. Although metabolic  
7 44 networks are generally highly resilient to perturbations, metabolic imbalance resulting from enzymatic  
8 45 defect and specific environmental conditions can be designed experimentally and studied. Starting with  
9 46 a double *amd1 aah1* mutant that severely and conditionally affects yeast growth, we carefully  
10 47 characterized the metabolic shuffle associated with this defect. We established that the GTP decrease  
11 48 resulting in an adenylic/guanylic nucleotide imbalance was responsible for the growth defect.  
12 49 Identification of several gene dosage suppressors revealed that *TAT1*, encoding an amino acid  
13 50 transporter, is a robust suppressor of the *amd1 aah1* growth defect. We show that *TAT1* suppression  
14 51 occurs through replenishment of the GTP pool in a process requiring the histidine biosynthesis pathway.  
15 52 Importantly, we establish that a *tat1* mutant exhibits synthetic-sickness when combined with an *amd1*  
16 53 mutant and that both components of this synthetic phenotype can be suppressed by specific gene dosage  
17 54 suppressors. Together our data point to a strong phenotypic connection between amino acid uptake and  
18 55 GTP synthesis, a connection that could open perspectives for future treatment of related human defects,  
19 56 previously reported as etiologically highly conserved.  
20  
21  
22  
23  
24  
25  
26 57  
27  
28 58  
29  
30

## 30 Introduction

31 60  
32 61 Metabolism is the highly integrated process of chemical interconversion in living organisms. It  
33 62 involves multiple enzymes organized in interconnected pathways. Although metabolic enzymes are  
34 63 generally highly specific and involved in a single pathway, mutations affecting metabolic enzymes can  
35 64 have multiple effects and result in complex phenotypes. Indeed, a simple block in a metabolic pathway,  
36 65 due to the lack of an enzyme activity, can have several effects such as, shortage of the product,  
37 66 accumulation of the substrate and/or imbalance between metabolites. All three features can contribute  
38 67 to the phenotype independently, additively or cooperatively and it is difficult to appraise their relative  
39 68 contribution which can vary in different tissues or during development (Daignan-Fornier and Pinson,  
40 69 2019). The use of simpler organisms to get a primary view of the metabolic consequences of the  
41 70 dysfunction has proved to be valuable, as for example in the case of AMP deaminase, which catalyzes  
42 71 synthesis of IMP from AMP and hence contributes to the Adenylic/Guanylic nucleotides balance (Fig.  
43 72 1). The yeast *amd1* mutant, lacking AMP deaminase, accumulates AMP the substrate of the reaction  
44 73 and its adenylic nucleotides derivatives (AXP), while it has low intracellular guanylic nucleotides (GXP)  
45 74 which are the physiological “end products” of the reaction (Saint-Marc et al., 2009). Addition of  
46 75 exogenous adenine to the growth medium is critical for the purine nucleotide imbalance and the growth  
47 76 defect associated with the *amd1* mutation (Saint-Marc et al., 2009). Strikingly, a similar purine  
48 77 nucleotide imbalance, dependent on adenylic precursors, was reported for *AMPD2* deficiency associated  
49 78 with a rare neurodegenerative disorder, pontocerebellar hypoplasia, in humans (Akizu et al., 2013). This  
50 79 remarkable conservation of a complex phenotype between yeast and human prompted us to take further  
51 80 advantage of yeast genetics to identify additional factors affecting the growth defect of the *amd1* mutant.  
52 81 In this work, we characterize mutations that modulate the phenotype of the *amd1* mutant and gene  
53 82 dosage suppressors that alleviate the growth defect associated with purine nucleotide imbalance in yeast.  
54  
55  
56  
57  
58  
59  
60  
61  
62  
63  
64  
65

83 These results revealed that, while the nucleotide imbalance due to the *amd1* mutation can be corrected  
1 84 through different means, no suppressors of effects downstream of the imbalance itself have been  
2 85 identified, hence indicating that this nucleotide imbalance most probably affects multiple physiological  
3 86 features and cannot easily be phenotypically circumvented.  
4  
5  
6 87

## 88 **Materials and Methods**

### 89 **Yeast media**

90  
91 SD is a synthetic minimal medium containing 0.5 % ammonium sulfate, 0.17 % yeast nitrogen base  
92 without amino acids and ammonium sulfate (BD-Difco; Franklin Lakes, NJ, USA) and 2 % glucose  
93 supplemented or not with adenine (0.3 mM) and/or histidine (0.09 mM) or uracil (0.3 mM; SDU).  
94 SDcasaW is SD medium supplemented with 0.2% casamino acids ((#A1404HA; Biokar/Solabia group;  
95 Pantin, France; this amino-acids mixture includes histidine at a final concentration of 0.3 mM in the  
96 medium) and tryptophan (0.2 mM). When indicated, adenine (0.3 mM), guanine (0.3 mM), histidine  
97 (0.09 mM), hypoxanthine (0.3 mM), and/or uracil (0.3 mM) were added in SDcasaW medium, resulting  
98 in media named SDcasaWA (+ adenine), SDcasaWHypox (+ hypoxanthine), SDcasaWAU (+ adenine  
99 + uracil), and SDcasaWU (+ uracil).  
100

### 101 **Yeast strains and plasmids**

102  
103 All yeast strains are listed in **Table 1** and belong to, or are derived from, a set of disrupted strains  
104 isogenic to BY4741 or BY4742 purchased from Euroscarf (Germany). Multi-mutant strains were  
105 obtained by crossing, sporulation and micromanipulation of meiosis progeny. The *amd1 aah1 apt1* triple  
106 mutant (Y11611) was obtained by disruption of *APT1* in Y2076 using an *APT1::URA3* cassette obtained  
107 by replacing the 433 bp *HindIII-HindIII* fragment of *APT1* (starting 158 bp after ATG) by a *HindIII-*  
108 *HindIII* fragment containing *URA* gene. All plasmids are listed in **Table 2**. Cloning details for the  
109 unpublished plasmids are available upon request.  
110

### 111 **Growth test**

112  
113 For drop tests, yeast cells from an overnight pre-culture were re-suspended in sterile water at  $1.10^7$   
114 cells/ml and submitted to 1/10 serial dilutions. Drops (5  $\mu$ l) of each dilution were spotted on freshly  
115 prepared medium plates and were incubated at 30 or 37 °C for 30–72 h before imaging.  
116

### 117 **Isolation of mutants and multicopy suppressors of the *amd1 aah1* and *amd1 tat1* adenine-** 118 **dependent growth defects.**

119  
120 Mutant suppressors of the *amd1 aah1* growth defect in the presence of adenine (Strain Y2076) were  
121 selected on SDcasaWUA medium after UV mutagenesis.

122 Multicopy suppressors of the *amd1 aah1* and *amd1 tat1* adenine-dependent growth defects were  
123 obtained by similar procedures. Yeast strains (Y2076 or Y11628) were transformed with a multicopy  
124 plasmid library (PFL44L backbone, 2 $\mu$  *URA3*; generous gift from F. Lacroute). Transformants were  
125 selected on SDcasaW medium and gene dosage suppressors were identified by replica-plating of the  
126 transformants on SDcasaWA medium and were then verified by drop test on both SDcasaW and  
127 SDcasaWA medium. For both multicopy suppressor screens, plasmids from selected clones were  
128 extracted and the genomic DNA region inserted in the plasmid was identified by sequencing. When the  
129

129 identified genomic region contained more than one open reading frame (ORF), each ORF was either  
1 130 subcloned individually or interrupted in the plasmid to unambiguously identify the gene responsible for  
2 131 suppression.

### 5 133 **Metabolite extraction and separation by liquid chromatography**

6 134  
7 135 Extraction of yeast metabolites was performed by the rapid filtration and ethanol boiling method as  
8 136 described (Loret et al., 2007) and metabolite separation was performed on an ICS3000 chromatography  
9 137 station (ThermoFisher) using a carbopac PA1 column (250 x 2 mm; ThermoFisher) with the 50 to 800  
10 138 mM sodium acetate gradient in NaOH 50 mM described in (Ceballos-Picot et al., 2015). Peaks were  
11 139 identified by their retention time as well as co-injection with standards and/or their UV spectrum  
12 140 signature (Ultimate-3000 diode array detector, ThermoFisher). Peak area quantifications were done at  
13 141 two different wavelengths: 260 nm for ADP, AMP, ATP, GTP, SAM and SAH and 269 nm for adenine  
14 142 and ZMP. AXP content corresponds to the sum of ATP + ADP + AMP contents. Adenylate energy  
15 143 charge was defined as  $AEC = (ATP + \frac{1}{2} ADP)/AXP$  (Atkinson and Walton, 1967). AXP and AEC were  
16 144 calculated with content of each nucleotide given in nmol/sample (inferred from standard curves using  
17 145 ATP, ADP and AMP pure compounds). For each measurement, presented in figures as mean with  
18 146 standard deviation, metabolic extractions were performed on independent cell cultures and  
19 147 normalization of samples was done on the basis of cell number and median cell volume (determined  
20 148 using a Multisizer 4 (Beckman Coulter)). Statistics were given as p-values determined by a Welch's  
21 149 unpaired t-test.

## 27 150 **RESULTS**

### 29 151 *The severe growth defect of the *amd1 aah1* mutant in the presence of adenine is due to GTP* 30 152 *shortage*

31 153  
32 154  
33 155 The *amd1* knock-out mutant grown in the presence of adenine showed a mild growth defect  
34 156 (Fig. 2a) accompanied by low GTP and high ATP (Saint-Marc et al., 2009). To enhance the growth  
35 157 phenotype and be able to achieve a suppressor screen, we combined *amd1* with the *aah1* knockout  
36 158 mutation, which further reduces the IMP-supply from adenine (Fig. 1). This genetic combination  
37 159 severely exacerbated the growth defect in the presence of adenine (Saint-Marc et al., 2009), but not in  
38 160 the presence of hypoxanthine that bypasses the lack of *aah1* or in the absence of added purines (Fig.2  
39 161 a). While metabolic profiling revealed no difference between the two strains in the absence of purines  
40 162 (Supplemental Fig. 1), the *amd1 aah1* mutant upon adenine feeding revealed several major metabolic  
41 163 changes (Fig.2 b-i) that could, either alone or combined, result in the observed growth phenotype. First,  
42 164 we found a severe reduction of intracellular GTP (Fig. 2b) and an increase of ATP (Fig. 2c) similar to  
43 165 what was previously reported for the *amd1* mutation alone (Saint-Marc et al., 2009), although more  
44 166 pronounced for GTP. Of note, in the *amd1 aah1* mutant, the sum of adenylic nucleotides ( $AXP = ATP$   
45 167 + ADP+ AMP) was increased (Fig. 2c-f), showing that the higher intracellular ATP is the result of net  
46 168 adenylic nucleotide synthesis and not merely of enhanced ADP to ATP interconversion. By contrast,  
47 169 adenylic energy charge ( $AEC = (ATP + \frac{1}{2} ADP)/AXP$ , Fig. 2g) was the same in the two strains grown  
48 170 in the presence of adenine, thus excluding an energetic defect as responsible for the *amd1 aah1* growth  
49 171 defect (Fig. 2a). In addition, we observed an important accumulation of S-adenosyl-methionine (SAM,  
50 172 Fig. 2h) and S-adenosyl-homocysteine (SAH, Fig. 2i), as previously reported for an *aah1* single mutant  
51 173 (Ceschin et al., 2015). Accumulation of SAH and SAM in the mutant are presumably due to inhibition  
52 174 of SAH hydrolase upon increased intracellular adenine (Fig. 2j)(Knudsen and Yall, 1972) and to  
53 175 inhibition of methyl-transferases by SAH (Zappia et al., 1969), respectively ( Fig.1, green dashed lines).  
54 176 We conclude that, in the *amd1 aah1* mutant, in the presence of external adenine, the steady state level

175 of several metabolites is strongly increased or decreased and we aimed at identifying more precisely  
1 176 which metabolites are responsible for growth impairment through targeted and non-targeted strategies.  
2

3 177 While SAM accumulation appears non-toxic for yeast cells (Roje et al., 2002), SAH  
4 178 accumulation was proposed to be toxic in a S-adenosyl-L-homocysteine hydrolase yeast mutant *sah1*  
5 179 (Christopher et al., 2002; Mizunuma et al., 2004; Visram et al., 2018) and could thus contribute to the  
6 179 growth defect of the *amd1 aah1* mutant. The potential role of SAH accumulation in the growth  
7 180 phenotype was assessed by two complementary approaches, the first one was designed to decrease SAH  
8 181 and the second one to increase it. First, we expressed the *E. coli* S-adenosylhomocysteine nucleosidase  
9 182 (*pfs*) enzyme in yeast to lower accumulation of SAM and SAH (Visram et al., 2018). As previously  
10 183 reported, expression of *pfs* suppressed the growth defect of *sah1-1* (Supplemental Fig. 2a) (Visram et  
11 184 al., 2018), but importantly it showed no suppressive effect on the growth defect of the *amd1 aah1* double  
12 185 mutant (Supplemental Fig. 2b). Metabolic profiling confirmed that *pfs* strongly decreased SAH and  
13 186 SAM in the *amd1 aah1* mutant (Supplemental Fig. 2c-d), indicating that high intracellular SAM and  
14 187 SAH in the *amd1 aah1* double mutant are not major causes in the growth defect in the presence of  
15 188 adenine. Of note, *pfs* had no effect on intracellular GTP that remained low (Supplemental Fig. 2e).  
16 189  
17 189  
18  
19  
20

21 190 Compared to the WT isogenic strain, the *amd1 aah1* mutant accumulated AXP (Fig. 2f) as well  
22 191 as SAM and SAH (Fig. 2h-i). To discriminate these metabolic effects, we combined the *aah1 amd1*  
23 192 mutant with an *apt1* mutant. In this triple mutant adenine cannot be used as a precursor anymore (Fig.  
24 192 1), but can exert its presumed inhibitory effect on Sah1 (Ceschin et al., 2015; Knudsen and Yall, 1972).  
25 193 We found that the growth defect of the *amd1 aah1* mutant on adenine was fully suppressed by a  
26 194 knockout of *APT1* (Fig. 3a) and that, in the triple *amd1 aah1 apt1* mutant, intracellular ATP was  
27 195 decreased (Fig. 3b) and GTP increased (Fig. 3c). In this mutant, intracellular adenine was increased, as  
28 196 expected due to the incapacity of the *amd1 aah1 apt1* mutant to use this metabolite (Fig. 3d) and, as  
29 197 anticipated, SAM and SAH were even higher than in the *amd1 aah1* double mutant (Fig. 3e-f). Together  
30 198 these results clearly establish that intracellular accumulation of SAM, SAH or adenine is not the cause  
31 199 of the growth defect of the *amd1 aah1* mutant and point to GTP (and possibly ATP) as the critical  
32 200 metabolite for the growth phenotype.  
33  
34 200  
35 201  
36

37 202 Finally, to address this issue with no *a priori*, we used a non-directed approach based on  
38 203 metabolic profiling of suppressors of the *amd1 aah1* growth defect obtained after UV mutagenesis. Four  
39 203 such suppressors, partially or totally restoring growth of the *amd1 aah1* mutant in the presence of  
40 204 adenine (Supplemental Fig. 3a), were further characterized by metabolic profiling (Supplemental Fig.  
41 205 3b-f). Clearly, all suppressors increased intracellular GTP (Supplemental Fig. 3b) and decreased ATP  
42 206 (Supplemental Fig. 3c), while SAM, SAH and/or adenine were either increased or decreased depending  
43 207 on the suppressor strain (Supplemental Fig. 3d-f). Thus, this non-directed suppressor strategy nicely  
44 208 confirmed the conclusions drawn from the above metabolite-targeted strategy. Of note, based on their  
45 209 metabolic profiles, we suspected that these suppressor mutations could be allelic to *FCY2* and *APT1* that  
46 209 block adenine uptake and its conversion to AMP (Fig. 1), respectively. These assumptions were  
47 210 validated by sequencing of these loci in the four suppressor strains as well as the corresponding control  
48 211 strain, revealing that the four suppressors correspond to three *fcy2* and one *apt1* mutants (see Table 1).  
49 211 The identity of the suppressors was further confirmed by complementation with the wild-type cognate  
50 212 genes carried on centromeric plasmids (Supplemental Fig. 3g).  
51 213  
52 213  
53 214  
54 215  
55

56 216 Based on these results, the low GTP / high ATP imbalance appeared to be the best candidate to  
57 217 account for *amd1 aah1* growth defect. Accordingly, guanine supplementation improved growth of the  
58 217 mutant in the presence of adenine although not restoring wild-type growth (Fig. 4a). However, when the  
59 218 same strains were grown in liquid medium for metabolic profiling experiments, we observed a complete  
60 219  
61  
62  
63  
64  
65

220 restoration of growth in the presence of adenine and guanine (Fig. 4b). This discrepancy could be due  
1 221 to the very poor solubility of guanine that could limit its diffusion on plates. Metabolic profiling in the  
2 222 presence of guanine confirmed a restoration, though partial, of intracellular GTP and ATP (Fig. 4c-d).  
3 223 From these results, we conclude that low intracellular GTP (possibly in combination with high ATP) is  
4 224 responsible for the growth defect of *amd1 aah1* mutant in the presence of adenine, while no significant  
5 225 role for accumulation of SAM or SAH could be established.  
6 226

### 226 ***Gene dosage suppressors refuel the GTP synthesis through de novo pathways***

227 To get further understanding on the causes of the *amd1 aah1* growth defect, we searched for  
10 227 gene-dosage suppressors that would restore growth of the *amd1 aah1* mutant in the presence of adenine.  
11 228 A yeast genomic multicopy plasmid library was transformed in the *amd1 aah1* mutant and 52  
12 229 transformants, showing improved capacity to grow in the presence of adenine, were studied. Among  
13 230 those, 20 plasmids contained either *AAH1* or *AMD1*, hence complementing one of the two mutations of  
14 231 the double mutant, and were not further studied. The remaining plasmids were extracted and  
15 232 retransformed in the *amd1 aah1* mutant and we could identify 15 plasmids that were clearly sufficient  
16 233 to restore growth of the *amd1 aah1* mutant in the presence of adenine. Eight plasmids contained a region  
17 234 of chromosome II carrying the *TAT1* gene as the only common entire coding region. Four plasmids  
18 235 contained a region carrying the *ADE4* gene and one carried the *HIS1* gene. One plasmid contained the  
19 236 *PIK1* gene alone and the last plasmid carried a region of chromosome IV containing three entire open  
20 237 reading frames (*RPL35B*, *RD11* and *PPH21*). Further experiments confirmed *TAT1*, *ADE4*, *HIS1*, *PIK1*  
21 238 and *PPH21* as the dosage suppressor genes (Fig. 5a-b). *TAT1* encodes an amino acid transporter, *ADE4*  
22 239 and *HIS1* encode the first enzymes of purine and histidine *de novo* pathways respectively, *PIK1* encodes  
23 240 a phosphatidylinositol 4-kinase and *PPH21* (with *PPH22*) encodes the catalytic subunit of protein  
24 241 phosphatase 2A, PP2A. *TAT1*, *HIS1* and *ADE4* were the strongest suppressors while *PIK1* and *PPH21*  
25 242 were both weak suppressors (Fig. 5a-b). Of note, *PIK1* suppression was more efficient at 30°C (Fig. 5a),  
26 243 while *PPH21* suppressed better at 37°C (Fig. 5b).  
27 244

245 The effect of each gene dosage suppressor on intracellular GTP was evaluated (Fig. 5c). *ADE4*  
34 245 and *HIS1* overexpression partially replenished intracellular GTP thus explaining their suppression effect  
35 246 most probably through fueling of IMP synthesis *via* the purine or histidine *de novo* pathway, respectively  
36 247 (Fig. 1). Indeed, both Ade4 and His1 have been shown previously to be controlling enzymes, tightly  
37 248 feedback inhibited by the end-products of the cognate pathways, ATP and histidine, respectively (Rasse-  
38 249 Messenguy and Fink, 1973; Rebora et al., 2001). The dual contribution of histidine and purine synthesis  
39 250 to the *amd1 aah1* growth phenotype was further established by the fact that concomitant repression of  
40 251 the two pathways by adenine and histidine was required to observe the *amd1 aah1* growth phenotype  
41 252 (Fig. 5d) as well as the intracellular GTP decrease (Fig. 5e). We conclude that GTP refueling *via*  
42 253 enhanced flux through the histidine or purine *de novo* pathway is sufficient to restore growth of the  
43 254 *amd1 aah1* mutant in good agreement with our previous observation of phenotypic suppression by  
44 255 exogenous guanine (Fig. 4). Of note, the gene dosage suppressors had no significant effect on  
45 256 intracellular ATP (Fig. 5f), indicating that intracellular GTP or the purine nucleotide balance is the  
46 257 critical factor responsible for the slow growth phenotype.  
47 258

### 259 ***The suppressor effect of TAT1, PIK1 and PPH21 overexpression requires a functional histidine pathway***

260  
261 *TAT1*, the strongest suppressor, had a mild, though highly significant, effect on GTP (Fig. 5c)  
262 suggesting that it could, at least in part, act *via* one or both the GTP refueling routes, namely *de novo*  
263 purine or histidine pathways. Clearly, *TAT1* overexpression had no suppressive effect in the *aah1 amd1*  
264  
265

264 *ade8 his1* strain blocking both the histidine and the purine *de novo* pathway (Fig. 6a). To discriminate  
1 265 between these two routes, *TAT1* was overexpressed in *amd1 ade4* and *amd1 his1* double mutants. In the  
2 266 *amd1 ade4* strain, *TAT1* was an efficient suppressor, while the suppression was totally abolished in the  
3 267 *amd1 his1* mutant (Fig. 6b). We conclude that suppression by *TAT1* overexpression requires a functional  
4 268 histidine biosynthesis pathway. This result suggests that *TAT1* overexpression (just as that of *HIS1*) acts  
5 269 by increasing the flux in the histidine pathway resulting in increased synthesis of ZMP (which is a by-  
6 270 product of histidine synthesis, Fig. 1) and a precursor of IMP and GMP synthesis (Fig. 1). Accordingly,  
7 271 in an *ade16 ade17* mutant background, blocking ZMP consumption and allowing to monitor its  
8 272 accumulation, we found that overexpression of *TAT1* increased ZMP in an *ade16 ade17*, as well as in  
9 273 an *ade16 ade17 ade8* but not in an *ade16 ade17 his1* mutants (Fig. 6c). From all these experiments, we  
10 274 conclude that *TAT1* acts as a suppressor by increasing the histidine pathway flux and thereby fueling the  
11 275 purine pathway *via* ZMP (Fig. 1). It is noteworthy that suppression due to *TAT1* overexpression was not  
12 276 dependent on the presence of the transcription factor Gcn4 that activates the histidine biosynthesis genes  
13 277 (Ljungdahl and Daignan-Fornier, 2012). Indeed, suppression by *TAT1* was similarly effective in the  
14 278 *amd1* and the *amd1 gcn4* mutants (Supplemental Fig. 4). Finally, as for *TAT1*, we found that suppression  
15 279 by overexpression of *PIK1* and *PPH21* required a functional histidine biosynthesis pathway (Fig. 6d).  
16 280 Hence, our results show that the three gene dosage suppressors *TAT1*, *PIK1* and *PPH21* act through the  
17 281 histidine pathway and suggest that they could participate to a common mechanism.

### 282 283 ***The amd1 tat1 double mutant shows a strong synthetic phenotype: identification of suppressors***

284 The results presented in the previous section established that *TAT1* overexpression interferes  
285 with purine nucleotide synthesis, and significantly on GTP, through the enhancement of the histidine  
286 pathway. Strikingly, our previous work had revealed that a *tat1* knockout mutation resulted in increased  
287 sensitivity to GTP shortage associated to treatment of yeast with mycophenolic acid (MPA) an  
288 immunosuppressive drug that operates by inhibiting IMP dehydrogenase (IMPDH) (Desmoucelles et  
289 al., 2002). Henceforth, overexpression of *TAT1* can suppress the GTP-shortage associated growth defect  
290 of the *amd1* and *amd1 aah1* mutants, while the lack of *tat1* rendered yeast cells more sensitive to GTP  
291 shortage. To examine further the relationship between Tat1 and GTP, we combined *tat1* and *amd1*  
292 mutations. As anticipated from increased MPA-sensitivity (Desmoucelles et al., 2002), the double  
293 mutant showed a synthetic growth defect specifically in the presence of adenine (Fig. 7a), when  
294 intracellular GTP is low in the *amd1* mutant. However, strikingly, this enhancement of the *amd1*  
295 phenotype by *tat1* was not associated to a further decrease of intracellular GTP, by contrast to what was  
296 observed for the *amd1 aah1* mutant combination (Fig. 7b). Hence, *TAT1* overexpression suppressed the  
297 growth defect of the *amd1 aah1* mutant by increasing intracellular GTP (Fig. 5c), while *tat1* mutation  
298 enhanced the *amd1* phenotype without further altering intracellular GTP (Fig. 7b). We conclude that  
299 *TAT1* over- and under-expression act through different means.

300 To examine further the synthetic growth phenotype of the *amd1 tat1* mutant, we isolated gene  
301 dosage suppressors that alleviate the growth defect of the double mutant in the presence of adenine. A  
302 set of 95 plasmids suppressing the growth defect of the *amd1 tat1* mutant were analyzed. Among those,  
303 45 carried the *TAT1* gene and 22 the *AMD1* gene, hence confirming that the phenotype is the result of  
304 the combination of the two mutations. The *bona fide* gene dosage suppressors include several genes  
305 involved in purine metabolism (*ADE4*, *AAH1*, *APT2*, *HPT1*, *XPT1*), but also the *PPH21* gene previously  
306 isolated in the *amd1 aah1* screen (see prior sections) and four new genes (*ERC1*, *HYM1*, *MSN2* and  
307 *BAP2*) exhibiting various suppression strength (Supplemental Fig. 5). Metabolic profiling of the  
308 suppressors (Fig. 7c) showed that most of them, excepting *MSN2*, *BAP2* and *HYM1*, significantly

309 increased intracellular GTP, suggesting that they act through replenishing IMP and GMP biosynthesis  
310 *via* the *de novo* pathway (*ADE4*) or the salvage pathway (*AAH1*, *HPT1*). *XPT1* was initially described  
311 as a gene dosage suppressor of *HPT1* (Guetsova et al., 1999) and could hence phenocopy *HPT1*  
312 overexpression for suppression of *amd1 tat1*. Two suppressors (*ERC1* and *HYM1*) increased  
313 intracellular SAH and SAM (Fig. 7d-e). In the case of *ERC1* this effect was very strong as previously  
314 reported (Kanai et al., 2017). *ERC1* encodes a member of the multi-drug and toxin extrusion family. It  
315 is not clear why its overexpression should suppress the *amd1 tat1* growth defect. However, the fact that  
316 the suppression by *ERC1* is associated to higher intracellular GTP, as well as higher SAM and SAH  
317 (Fig. 7c-e), confirmed that accumulation of the latter two metabolites is not involved in the mutant  
318 growth phenotype.

319 The identification of *APT2* as a gene dosage suppressor of *amd1 tat1* was quite surprising since  
320 *Apt2* is presumed to have no APRT activity (Alfonzo et al., 1999) and that, in any case, overexpression  
321 of APRT rather exacerbated than improved the growth phenotype of the *amd1* mutant (Saint-Marc et  
322 al., 2009). Indeed, overexpression of the two paralogues, *APT1* and *APT2*, had opposite effects on the  
323 growth of *amd1* in the presence of adenine, while *APT2* overexpression clearly suppressed *amd1*; *APT1*  
324 enhanced its growth defect (Fig. 7f). Whether suppression by *APT2* was dependent on *Apt1* was tested  
325 in an *amd1 apt1 tat1* triple mutant (Supplemental Fig. 6) but no conclusion could be drawn since *amd1*  
326 *tat1* was robustly suppressed by *apt1*, similarly to what we found previously for *aah1 amd1* (Fig. 3A)  
327 Thus, we conclude that *APT2* rather counteracts than mimics *APT1* phenotypically. Of note, in the BY  
328 background, *apt2* was neither synthetic lethal with *apt1* (Supplemental Fig. 7) nor *aah1* (Supplemental  
329 Fig. 8), by contrast to what was reported in SGD database based on a genome-wide analysis (Deutscher  
330 et al., 2006).

## 331 332 DISCUSSION

### 333 *Deciphering the precise metabolic defect responsible for the growth phenotype*

334 This work illustrates how simple metabolic blocks can result in conditional accumulation or defect of  
335 multiple metabolites. This complex profile is due to the untangled architecture of the metabolic network,  
336 which favors robustness but makes phenotypic interpretation difficult. Yeast genetics clearly allowed  
337 addressing separately the contribution of these metabolites to the growth phenotype. Interestingly, a  
338 metabolite such as SAH, supposedly highly toxic, accumulated under conditions of robust growth (for  
339 example *amd1 aah1 apt1* mutant Fig. 3) suggesting that combinations of faulty metabolites, rather than  
340 a single defect, are contributing to the phenotypic outcome making it difficult to understand completely.  
341 This work exemplifies, in a very simple isogenic situation, the complex interplay between pleiotropy  
342 (several metabolites affected and most probably several downstream functions impaired) and external  
343 conditions (presence of various purine precursors at constantly varying concentrations in the cellular  
344 environment, variable suppression efficiency depending on temperature, liquid versus solid medium... ).  
345 It therefore strongly questions our future capability to predict accurately phenotype from genotype.

### 346 *Suppression patterns suggest pleiotropy*

347 Strikingly, all the suppressors of the *amd1 aah1* growth defect in the presence of adenine restored at  
348 least partially GTP and the ATP/GTP balance, hence confirming that it is most likely causative of the  
349 growth phenotype. The fact that no suppressors were found restoring functionally downstream processes  
350 that could be affected by low GTP or purine imbalance, strongly suggests that there is not a single  
351 limiting factor but, instead, that the metabolic defect is most probably pleiotropic. A serious candidate-

352 function is protein translation that was found altered in a yeast *gual* mutant limiting GMP synthesis  
1 353 from IMP (Iglesias-Gato et al., 2011) and also in *amd1* and human *AMPD2* defective cells (Akizu et al.,  
2 354 2013). However, GTP is required at many steps in the translation process and our suppressor screen did  
3 355 not point to any single critical step. Our results rather suggest that replenishment of the GTP pool and/or  
4 356 GTP/ATP balance should be the target of future treatments.

### 7 357 ***TAT1 is tightly connected to intracellular GTP***

9 358 *TAT1* was identified as a robust gene dosage suppressor and its suppression ability was clearly dependent  
10 359 on the histidine synthesis pathway. The precise mechanism is unknown but *TAT1* overexpression  
11 360 strongly stimulated ZMP synthesis when the histidine pathway was the only possible route (in the *ade8*  
12 361 *ade16 ade17* mutant Fig. 6c). This connection, between an amino acid transporter, which is not a major  
13 362 histidine carrier, and the histidine biosynthesis pathway is intriguing. We found that suppression due to  
14 363 *TAT1* overexpression was not dependent on the presence of Gcn4 which is a major transcription factor  
15 364 involved in expression of the histidine biosynthesis genes (Ljungdahl and Daignan-Fornier, 2012). The  
16 365 mechanism connecting *TAT1* to the histidine pathway remains to be clarified but is complicated by the  
17 366 fact that *tat1* knock-out interferes with *amd1* through a different mean. Indeed, our previous work  
18 367 revealed an exacerbated sensitivity of the *tat1* knock-out mutant to mycophenolic acid, a specific  
19 368 inhibitor of GTP synthesis (Desmoucelles et al., 2002). Here we found that the *amd1* mutant was  
20 369 synthetic sick with *tat1* specifically in the presence of adenine leading to low intracellular GTP.  
21 370 However, by contrast to synthetic sickness of *amd1* with *aah1*, *tat1* did not exacerbate the intracellular  
22 371 GTP defect. Gene dosage suppressors revealed that there are two ways to suppress this growth defect.  
23 372 Either by replenishing the GTP pool by overexpression of purine interconversion genes, or by  
24 373 overexpressing the amino acid transporter Bap2 (Fig. 7). Together our data point to a strong phenotypic  
25 374 connection between amino acid uptake and GTP synthesis.

31 375 Interestingly, *PIK1* another gene dosage suppressor identified in this work also requires a fully  
32 376 functional histidine pathway to suppress the *aah1 amd1* growth phenotype. The link between this  
33 377 inositol kinase and GTP synthesis is potentially highly relevant since another inositol kinase was shown  
34 378 to sense GTP and respond to it (Sumita et al., 2016). Identifying further connections between guanine  
35 379 nucleotides and inositol derivatives could prove to be physiologically very important considering the  
36 380 key roles played by these metabolites.

### 40 381 ***What function for APT2?***

42 382 Suppression of the *amd1 tat1* mutant revealed gene dosage suppressors that increase intracellular GTP  
43 383 and others, such as *BAP2*, that probably partially compensate for the *tat1* defect. Among suppressors  
44 384 partially restoring intracellular GTP, most can be interpreted as redirecting adenine to IMP via  
45 385 hypoxanthine (*AAH1*, *HPT1*, *XPT1*) or via the purine *de novo* pathway (*ADE4*) (Fig. 1). Among these  
46 386 suppressor genes, identification of *APT2* was surprising. *APT2* does not code for functional APRT  
47 387 (Alfonzo et al., 1999) and in any case, *APT1* overexpression enhances the *amd1* phenotype while *APT2*  
48 388 was a gene dosage suppressor (Fig. 7f). Our results hence rather indicate that *APT2* antagonizes *APT1*  
49 389 as was previously proposed (Carlsson et al., 2018). This situation is remindful of what we reported for  
50 390 Ybr284w and Yjl070c, two paralogs of Amd1, that, when overexpressed, were shown to mimic *amd1*  
51 391 knockout (Saint-Marc et al., 2009). Hence, the fact that paralogs can antagonize each other could be a  
52 392 recurrent feature of metabolism in yeast.

### 57 393 ***Concluding remark***

394 In a more general perspective, understanding the effects of GTP deprivation and ATP/GTP imbalance  
1 395 could be of great value to understand how purine biosynthesis and interconversion affect complex  
2 396 diseases such as for example cancer. Indeed nucleotides are central in cancer cell metabolism but their  
3 397 dual roles as energy suppliers and building blocks are difficult to separate (Vander Heiden and  
4 398 DeBerardinis, 2017). In yeast, the effects of GTP deprivation and ATP/GTP imbalance on gene  
5 399 expression have been explored and proved complex (Hesketh et al., 2019; Saint-Marc et al., 2009). The  
6 400 high pleiotropy, due to the central role of these metabolites in multiple key processes within the cell,  
7 401 makes it difficult to address experimentally, but yeast has proved to be a good model to tackle this  
8 402 problem (Hesketh and Oliver, 2019).

## 403 404 **References**

- 16 405 Akizu, N., Cantagrel, V., Schroth, J., Cai, N., Vaux, K., McCloskey, D., Naviaux, R.K., Van Vleet, J.,  
17 406 Fenstermaker, A.G., Silhavy, J.L., *et al.* (2013). AMPD2 regulates GTP synthesis and is mutated in a  
18 407 potentially treatable neurodegenerative brainstem disorder. *Cell* 154, 505-517.
- 19 408 Alfonzo, J.D., Crother, T.R., Guetsova, M.L., Daignan-Fornier, B., and Taylor, M.W. (1999). APT1, but  
20 409 not APT2, codes for a functional adenine phosphoribosyltransferase in *Saccharomyces cerevisiae*. *J*  
21 410 *Bacteriol* 181, 347-352.
- 22 411 Atkinson, D.E., and Walton, G.M. (1967). Adenosine triphosphate conservation in metabolic regulation.  
23 412 Rat liver citrate cleavage enzyme. *J Biol Chem* 242, 3239-3241.
- 24 413 Bonneaud, N., Ozier-Kalogeropoulos, O., Li, G.Y., Labouesse, M., Minvielle-Sebastia, L., and Lacroute,  
25 414 F. (1991). A family of low and high copy replicative, integrative and single-stranded *S. cerevisiae*/E.  
26 415 *coli* shuttle vectors. *Yeast* 7, 609-615.
- 27 416 Carlsson, M., Hu, G.Z., and Ronne, H. (2018). Gene dosage effects in yeast support broader roles for  
28 417 the LOG1, HAM1 and DUT1 genes in detoxification of nucleotide analogues. *PLoS One* 13, e0196840.
- 29 418 Ceballos-Picot, I., Le Dantec, A., Brassier, A., Jais, J.P., Ledroit, M., Cahu, J., Ea, H.K., Daignan-Fornier,  
30 419 B., and Pinson, B. (2015). New biomarkers for early diagnosis of Lesch-Nyhan disease revealed by  
31 420 metabolic analysis on a large cohort of patients. *Orphanet J Rare Dis* 10, 7.
- 32 421 Ceschin, J., Hurlimann, H.C., Saint-Marc, C., Albrecht, D., Violo, T., Moenner, M., Daignan-Fornier, B.,  
33 422 and Pinson, B. (2015). Disruption of Nucleotide Homeostasis by the Antiproliferative Drug 5-  
34 423 Aminoimidazole-4-carboxamide-1-beta-d-ribofuranoside Monophosphate (AICAR). *J Biol Chem*  
35 424 290, 23947-23959.
- 36 425 Christopher, S.A., Melnyk, S., James, S.J., and Kruger, W.D. (2002). S-adenosylhomocysteine, but not  
37 426 homocysteine, is toxic to yeast lacking cystathionine beta-synthase. *Mol Genet Metab* 75, 335-343.
- 38 427 Daignan-Fornier, B., and Pinson, B. (2019). Yeast to Study Human Purine Metabolism Diseases. *Cells* 8.
- 39 428 Desmoucelles, C., Pinson, B., Saint-Marc, C., and Daignan-Fornier, B. (2002). Screening the yeast  
40 429 "disruptome" for mutants affecting resistance to the immunosuppressive drug, mycophenolic acid.  
41 430 *J Biol Chem* 277, 27036-27044.
- 42 431 Deutscher, D., Meilijson, I., Kupiec, M., and Ruppin, E. (2006). Multiple knockout analysis of genetic  
43 432 robustness in the yeast metabolic network. *Nat Genet* 38, 993-998.
- 44 433 Gari, E., Piedrafita, L., Aldea, M., and Herrero, E. (1997). A set of vectors with a tetracycline-regulatable  
45 434 promoter system for modulated gene expression in *Saccharomyces cerevisiae*. *Yeast* 13, 837-848.
- 46 435 Gietz, R.D., and Sugino, A. (1988). New yeast-*Escherichia coli* shuttle vectors constructed with in vitro  
47 436 mutagenized yeast genes lacking six-base pair restriction sites. *Gene* 74, 527-534.
- 48 437 Guetsova, M.L., Crother, T.R., Taylor, M.W., and Daignan-Fornier, B. (1999). Isolation and  
49 438 characterization of the *Saccharomyces cerevisiae* XPT1 gene encoding xanthine phosphoribosyl  
50 439 transferase. *J Bacteriol* 181, 2984-2986.
- 51 440 Hesketh, A., and Oliver, S.G. (2019). High-energy guanine nucleotides as a signal capable of linking  
52 441 growth to cellular energy status via the control of gene transcription. *Curr Genet* 65, 893-897.

442 Hesketh, A., Vergnano, M., and Oliver, S.G. (2019). Determination of the Global Pattern of Gene  
1 443 Expression in Yeast Cells by Intracellular Levels of Guanine Nucleotides. *mBio* 10.  
2 444 Iglesias-Gato, D., Martin-Marcos, P., Santos, M.A., Hinnebusch, A.G., and Tamame, M. (2011). Guanine  
3 445 nucleotide pool imbalance impairs multiple steps of protein synthesis and disrupts GCN4  
4 446 translational control in *Saccharomyces cerevisiae*. *Genetics* 187, 105-122.  
5 447 Kanai, M., Kawata, T., Yoshida, Y., Kita, Y., Ogawa, T., Mizunuma, M., Watanabe, D., Shimoj, H., Mizuno,  
6 448 A., Yamada, O., *et al.* (2017). Sake yeast YHR032W/ERC1 haplotype contributes to high S-  
7 449 adenosylmethionine accumulation in sake yeast strains. *J Biosci Bioeng* 123, 8-14.  
8 450 Knudsen, R.C., and Yall, I. (1972). Partial purification and characterization of S-adenosylhomocysteine  
9 451 hydrolase isolated from *Saccharomyces cerevisiae*. *J Bacteriol* 112, 569-575.  
10 452 Ljungdahl, P.O., and Daignan-Fornier, B. (2012). Regulation of amino acid, nucleotide, and phosphate  
11 453 metabolism in *Saccharomyces cerevisiae*. *Genetics* 190, 885-929.  
12 454 Loret, M.O., Pedersen, L., and Francois, J. (2007). Revised procedures for yeast metabolites extraction:  
13 455 application to a glucose pulse to carbon-limited yeast cultures, which reveals a transient activation  
14 456 of the purine salvage pathway. *Yeast* 24, 47-60.  
15 457 Mizunuma, M., Miyamura, K., Hirata, D., Yokoyama, H., and Miyakawa, T. (2004). Involvement of S-  
16 458 adenosylmethionine in G1 cell-cycle regulation in *Saccharomyces cerevisiae*. *Proc Natl Acad Sci U S*  
17 459 *A* 101, 6086-6091.  
18 460 Pinson, B., Vaur, S., Sagot, I., Couplier, F., Lemoine, S., and Daignan-Fornier, B. (2009). Metabolic  
19 461 intermediates selectively stimulate transcription factor interaction and modulate phosphate and  
20 462 purine pathways. *Genes Dev* 23, 1399-1407.  
21 463 Rasse-Messenguy, F., and Fink, G.R. (1973). Feedback-resistant mutants of histidine biosynthesis in  
22 464 yeast. *Basic Life Sci* 2, 85-95.  
23 465 Rebora, K., Desmoucelles, C., Borne, F., Pinson, B., and Daignan-Fornier, B. (2001). Yeast AMP pathway  
24 466 genes respond to adenine through regulated synthesis of a metabolic intermediate. *Mol Cell Biol*  
25 467 21, 7901-7912.  
26 468 Rebora, K., Laloo, B., and Daignan-Fornier, B. (2005). Revisiting purine-histidine cross-pathway  
27 469 regulation in *Saccharomyces cerevisiae*: a central role for a small molecule. *Genetics* 170, 61-70.  
28 470 Roje, S., Chan, S.Y., Kaplan, F., Raymond, R.K., Horne, D.W., Appling, D.R., and Hanson, A.D. (2002).  
29 471 Metabolic engineering in yeast demonstrates that S-adenosylmethionine controls flux through the  
30 472 methylenetetrahydrofolate reductase reaction in vivo. *J Biol Chem* 277, 4056-4061.  
31 473 Saint-Marc, C., Pinson, B., Couplier, F., Jourden, L., Lisova, O., and Daignan-Fornier, B. (2009).  
32 474 Phenotypic consequences of purine nucleotide imbalance in *Saccharomyces cerevisiae*. *Genetics*  
33 475 183, 529-538, 521SI-527SI.  
34 476 Sumita, K., Lo, Y.H., Takeuchi, K., Senda, M., Kofuji, S., Ikeda, Y., Terakawa, J., Sasaki, M., Yoshino, H.,  
35 477 Majd, N., *et al.* (2016). The Lipid Kinase PI5P4Kbeta Is an Intracellular GTP Sensor for Metabolism  
36 478 and Tumorigenesis. *Mol Cell* 61, 187-198.  
37 479 Vander Heiden, M.G., and DeBerardinis, R.J. (2017). Understanding the Intersections between  
38 480 Metabolism and Cancer Biology. *Cell* 168, 657-669.  
39 481 Visram, M., Radulovic, M., Steiner, S., Malanovic, N., Eichmann, T.O., Wolinski, H., Rechberger, G.N.,  
40 482 and Tehlivets, O. (2018). Homocysteine regulates fatty acid and lipid metabolism in yeast. *J Biol*  
41 483 *Chem* 293, 5544-5555.  
42 484 Zappia, V., Zydek-Cwick, R., and Schlenk, F. (1969). The specificity of S-adenosylmethionine derivatives  
43 485 in methyl transfer reactions. *J Biol Chem* 244, 4499-4509.

44 486  
45  
46 487

47  
48  
49  
50  
51  
52  
53  
54  
55  
56  
57  
58  
59  
60  
61  
62  
63  
64  
65

488 **Figure legends**

1  
2 489  
3 490 **Fig. 1** Schematic representation of the *de novo* purine and histidine pathways and of the methyl cycle in  
4 491 yeast. Only the enzymes mentioned in the text are shown (in red). *AMP* adenosine 5'-monophosphate,  
5 492 *GMP* Guanosine 5'-monophosphate, *IMP* Inosine 5'-monophosphate, *PRFZMP* N-5-phosphoribosyl-  
6 493 formimino-5-amino-imidazole-4-carboxamide ribonucleotide monophosphate, *PRPP*  $\alpha$ -D-ribofuranose  
7 494 5-phosphate 1-diphosphate, *SAH* S-adenosyl-L-homocysteine, *SAM* S-adenosyl-L-methionine, *XMP*  
8 495 xanthosine 5'-monophosphate and *ZMP* 5-amino-imidazole 4-carboxamide ribonucleotide 5'-  
9 496 monophosphate (also known as AICAR monophosphate). The dashed green lines show the inhibition of  
10 497 the S-adenosyl homocysteine hydrolase activity by adenine and of the methyl-transferases by S-  
11 498 adenosyl-L-homocysteine (see text).  
12  
13  
14  
15 499

16 500  
17 501 **Fig. 2** Growth alteration of the *amd1 aah1* double mutant in the presence of adenine is associated with  
18 502 changes in the steady state level of several purine derivatives. **a** Adenine supplementation strongly  
19 503 affects proliferation of an *amd1 aah1* double mutant. Yeast cells (Y175, Y2076, Y4198 and Y6750)  
20 504 were serially diluted and grown for 48 hours at 30°C on SDcasaWU medium supplemented or not with  
21 505 indicated purines. **b-j** Metabolic changes associated to adenine supplementation in the *amd1 aah1*  
22 506 double mutant. Y175 (wild-type (WT), blue dots) and Y2076 (red dots) were exponentially grown for  
23 507 24 h in SDcasaWU and adenine was added for 4 h before metabolic extraction. Metabolites were then  
24 508 separated by liquid chromatography, quantifications were determined on biologically independent  
25 509 extractions and standard deviation is presented. For each metabolite, the amount measured in wild-type  
26 510 cells (blue dots) was set at 1. Numbers on the top of each panel correspond to the p-value calculated  
27 511 from a Welch's unpaired t-test. **h-j** the dashed blue line illustrates scale breaks. **a-j** Of note, media used  
28 512 in this figure contains 0.3 mM of histidine from the casamino-acids mixture.  
29  
30  
31  
32  
33 513

34 514 **Fig. 3** Deletion of *APT1* is sufficient to restore both proliferation and intracellular purine nucleotide  
35 515 triphosphate level in the *amd1 aah1* mutant. **a** The adenine-dependent growth defect of the *amd1 aah1*  
36 516 mutant was fully suppressed by *APT1* knockout. Dilutions of BY4742 (wild-type), Y2076 and Y11611  
37 517 strains were spotted on SDcasaWU medium (containing 0.3 mM of histidine) supplemented or not with  
38 518 adenine and grown for 40 h at 30°C. **b-f** Restoration of ATP and GTP levels by deletion of *APT1*. Strains  
39 519 (Y2076 and Y11611) were grown in SDcasaWU medium and adenine was added for 4 h before  
40 520 metabolic extraction, separation and quantification done as in Fig. 2. For each metabolite, the amount  
41 521 measured in the *amd1 aah1* cells was set at 1 (red dots). Numbers on the top of each panel correspond  
42 522 to the p-value calculated from a Welch's unpaired t-test.  
43  
44  
45  
46 523

47 524 **Fig. 4** Alteration of *amd1 aah1* proliferation by adenine is alleviated by guanine supplementation and is  
48 525 associated to a partial restoration of the GTP/ATP imbalance. **a-b** Guanine supplementation suppresses  
49 526 either partially on plates (**a**) or totally in liquid (**b**) the proliferation defect of the *amd1 aah1* mutant. **a**  
50 527 BY4741 (wild-type) and Y2076 strains were serially diluted and grown for 30 hours at 30°C on  
51 528 SDcasaWU medium supplemented or not with indicated purines. **b** The *amd1 aah1* mutant (Y2076) was  
52 529 exponentially grown for 24 hours in SDcasaWU and diluted to  $2 \times 10^6$  cells/ml in the same medium  
53 530 containing or not adenine (green and blue dots) and guanine (blue dots). Cell proliferation was followed  
54 531 using a Multisizer IV (Beckman Coulter). **c-d** ATP (**c**) and GTP (**d**) relative contents are partially  
55 532 restored under guanine supplementation. Metabolic extraction, separation and quantification were done  
56 533 as in Fig. 2 on the *amd1 aah1* mutant shifted (Y2076) for 4 h to SDcasaWU medium supplemented or  
57 534 not (red dots) with adenine (green dots) or adenine + guanine (blue dots). For each metabolite, the  
58  
59  
60  
61  
62  
63  
64  
65

535 amount measured in cells grown in the absence of purine (red dots) was set at 1. Numbers correspond  
1 536 to the p-value calculated from a Welch's unpaired t-test.

2 537  
3  
4 538 **Fig. 5** Gene dosage suppressors alleviate the adenine-dependent growth defect of the *amd1 aah1* mutant  
5 539 in a GTP-refueling dependent manner. **a-c, f** Wild-type (WT, Y175) and *amd1 aah1* (Y2076) strains  
6 540 were transformed with plasmids allowing overexpression (OE) or not (None) of indicated genes (p5839,  
7 541 p5840, p5841, p5842 and p5847 for *TAT1*, *PIK1*, *ADE4*, *HIS1* and *PPH21*, respectively). **a-b**  
8 542 Transformants were serially diluted and grown for 48 h on SDcasaW medium (containing 0.3 mM of  
9 543 histidine (His) from casamino-acids) supplemented or not with adenine (Ade) at 30 °C (**a**) and 37°C (**b**).  
11 544 **c** GTP relative level is increased in most of the gene dosage suppressors. Transformants were  
12 545 exponentially grown for 24 h in SDcasaW medium and then adenine was added for 4 h before metabolite  
13 546 extraction. The amount of GTP measured in wild-type cells transformed by the control plasmid (None,  
14 547 blue dots) was set at 1. **d-e** Histidine and purine pathways are both required to observe a growth defect  
15 548 and a GTP drop in the *amd1 aah1* mutant. **d** Y2076 strain was transformed with the *HIS3 LEU2*  
16 549 centromeric plasmid (p2191, which renders it prototrophic for histidine) and with plasmids allowing  
17 550 overexpression of either *HIS1* (p3332) or *ADE4* (p1933) genes or by the cognate control vectors (None,  
18 551 pCM189 or PFL44L). Serial dilutions were spotted on SD medium ± Adenine (0.3 mM) ± Histidine  
19 552 (0.09 mM) and plates were imaged after 48 h at 30°C. **e** The *amd1 aah1* mutant (Y2076) containing the  
20 553 *HIS3 LEU2* plasmid was exponentially grown for 24 h in SDU medium and then GTP levels were  
21 554 determined after a 4 h incubation in the presence or absence of adenine and/or histidine. The amount of  
22 555 GTP measured in cells grown in the absence of supplement (No addition) was set at 1. **f** ATP relative  
23 556 content determined in the metabolic extracts from Fig. 5c. **c, e-f** Numbers correspond to the p-value  
24 557 calculated from a Welch's unpaired t-test.

25 558  
26 559 **Fig. 6** A functional histidine pathway is required for the gene dosage suppression of the *amd1*  
27 560 proliferation phenotype. **a-b** Suppression of the *amd1 aah1* growth phenotype by *TAT1* overexpression  
28 561 is inoperative in the absence of histidine pathway. Yeast strains (Y2690, Y11779, Y11784 and Y11821)  
29 562 were transformed with a plasmid allowing *TAT1* overexpression (OE, p5839) or by the empty vector  
30 563 (None, pFL44L). Transformants were grown for 48 h at 30 °C on SDcasaW medium containing 0.3 mM  
31 564 of histidine (from casamino-acids) and the indicated source of purine. **c** *TAT1* overexpression results in  
32 565 an increased level of ZMP synthesized from the histidine pathway. Yeast (Y1162, Y2787 and Y4423)  
33 566 were transformed with the *TAT1* overexpression plasmid or the cognate empty vector (None). ZMP level  
34 567 were determined on cells grown in SDcasaWA medium as described in Fig. 2. The amount measured in  
35 568 *ade16 ade17* cells with the empty vector (light orange dots) was set at 1. Numbers correspond to the p-  
36 569 value calculated from a Welch's unpaired t-test. **d** A functional histidine pathway is required for  
37 570 suppressor effect of *PPH21* and *PIK1* on *amd1* mutant proliferation. Y11643, Y11782 and Y11821  
38 571 yeast strains were transformed with an empty vector (None, PFL44L) or with plasmids overexpressing  
39 572 (OE) the indicated genes (p5839, p5840 and p5847). Transformants were grown for 48 h at 30°C on  
40 573 SDcasaW medium containing the indicated source of purine.

41 574  
42 575 **Fig. 7** Suppressors effect on the proliferation and metabolic phenotypes associated with the *amd1 tat1*  
43 576 mutant. **a-b** The *amd1 tat1* double mutant displays a severe growth defect but not associated to an  
44 577 enhanced GTP decrease compared to *amd1*. Yeast strains (BY4742 (wild-type), Y1031, Y2076 and  
45 578 Y11627) were serially diluted and grown for 48 h at 30°C on SDcasaWU medium (containing 0.3 mM of  
46 579 histidine from casamino-acids) supplemented or not with adenine (**a**) or were exponentially grown in  
47 580 SDcasaWU medium for 24 h and adenine was added 4 h before being submitted to a metabolic extraction  
48 581 and GTP quantification as in Fig. 2 (**b**). GTP level determined in wild type cells (blue dots) was set at  
49 582 1. **c-e** Metabolic profiling of the *amd1 tat1* gene-dosage suppressors. The *amd1 tat1* double mutant strain

583 was transformed with plasmids overexpressing (OE) the indicated genes (p5894, p5896, p5897, p5898,  
1 584 p5899, p5900, p5901, p5902 and p6026 for *XPT1*, *ADE4*, *HYM1*, *ERC1*, *MSN2*, *BAP2*, *AAH1*, *HPT1*  
2 585 and *APT2* or by the empty vector (None, pFL44L). Transformants were exponentially grown for 24 h  
3 586 in SDcasaWU medium, adenine was then added for 4 h prior to metabolic extraction as in Fig. 2. For  
4 587 each metabolite, the level determined in cells containing the empty vector (orange dots) was set at 1. **b-**  
5 588 **e** Numbers correspond to the p-value calculated from a Welch's unpaired t-test. **f** Growth of *amd1* in  
6 589 the presence of adenine is restored by overexpression of *APT2* but not *APT1*. The *amd1* mutant  
7 590 (Y11784) was transformed by plasmids allowing overexpression of *APT1* (p5011) or *APT2* (p552) or  
8 591 by the empty vector (None, YepLac195). Transformants were serial diluted and growth was imaged  
9 592 after 48 h at 30°C on SDcasaW medium ± adenine.  
10 593

<b>Table 1</b> Yeast strains used in this study		
Strain	Genotype	References
BY4741	<i>MATa his3Δ1 leu2Δ0 ura3Δ0 met15Δ0</i>	Euroscarf
BY4742	<i>MATα his3Δ1 leu2Δ0 ura3Δ0 lys2Δ0</i>	Euroscarf
Y175	<i>MATa his3Δ1 leu2Δ0 ura3Δ0</i>	This study
Y1031	<i>MATa his3Δ1 leu2Δ0 ura3Δ0 met15Δ0 amd1::KanMX4</i>	Euroscarf
Y1162	<i>MATα his3Δ1 leu2Δ0 ura3Δ0 ade16::KanMX4 ade17::KanMX4</i>	(Pinson et al., 2009)
Y2076	<i>MATa his3Δ1 leu2Δ0 ura3Δ0 aah1::KanMX4 amd1::KanMX4</i>	This study
Y2690	<i>MATα his3Δ1 leu2Δ0 lys2Δ0 ura3Δ0 aah1::KanMX4 amd1::KanMX4 ade8::KanMX4 his1::KanMX4</i>	This study
Y2787	<i>MATa his3Δ1 leu2Δ0 ura3Δ0 met15Δ0 his1::KanMX4 ade16::KanMX4 ade17::KanMX4</i>	(Pinson et al., 2009)
Y4198	<i>MATa his3Δ1 leu2Δ0 ura3Δ0 amd1::KanMX4</i>	This study
Y4423	<i>MATa his3Δ1 leu2Δ0 ura3Δ0 ade8::KanMX4 ade16::KanMX4 ade17::KanMX4</i>	This study
Y5941	<i>MATa trp1 leu2 ade2 ura3 his3 can1-100 sah1-1</i>	(Mizunuma et al., 2004)
Y6750	<i>MATa his3Δ1 leu2Δ0 ura3Δ0 aah1::KanMX4</i>	(Ceschin et al., 2015)
Y11611	<i>MATa his3Δ1 leu2Δ0 ura3Δ0 aah1::KanMX4 amd1::KanMX4 apt1::URA3</i>	This study
Y11627	<i>MATa his3Δ1 leu2Δ0 ura3Δ0 lys2Δ0 met15Δ0 tat1::KanMX4 amd1::KanMX4</i>	This study
Y11643	<i>MATa his3Δ1 ura3Δ0 amd1::KanMX4</i>	This study
Y11779	<i>MATa ura3Δ0 ade4::KanMX4 amd1::KanMX4</i>	This study
Y11782	<i>MATa ura3Δ0 leu2Δ0 ade4::KanMX4 amd1::KanMX4</i>	This study
Y11784	<i>MATa ura3Δ0 amd1::KanMX4</i>	This study
Y11821	<i>MATα his3Δ1 leu2Δ0 ura3Δ0 his1::KanMX4 amd1::KanMX4</i>	This study

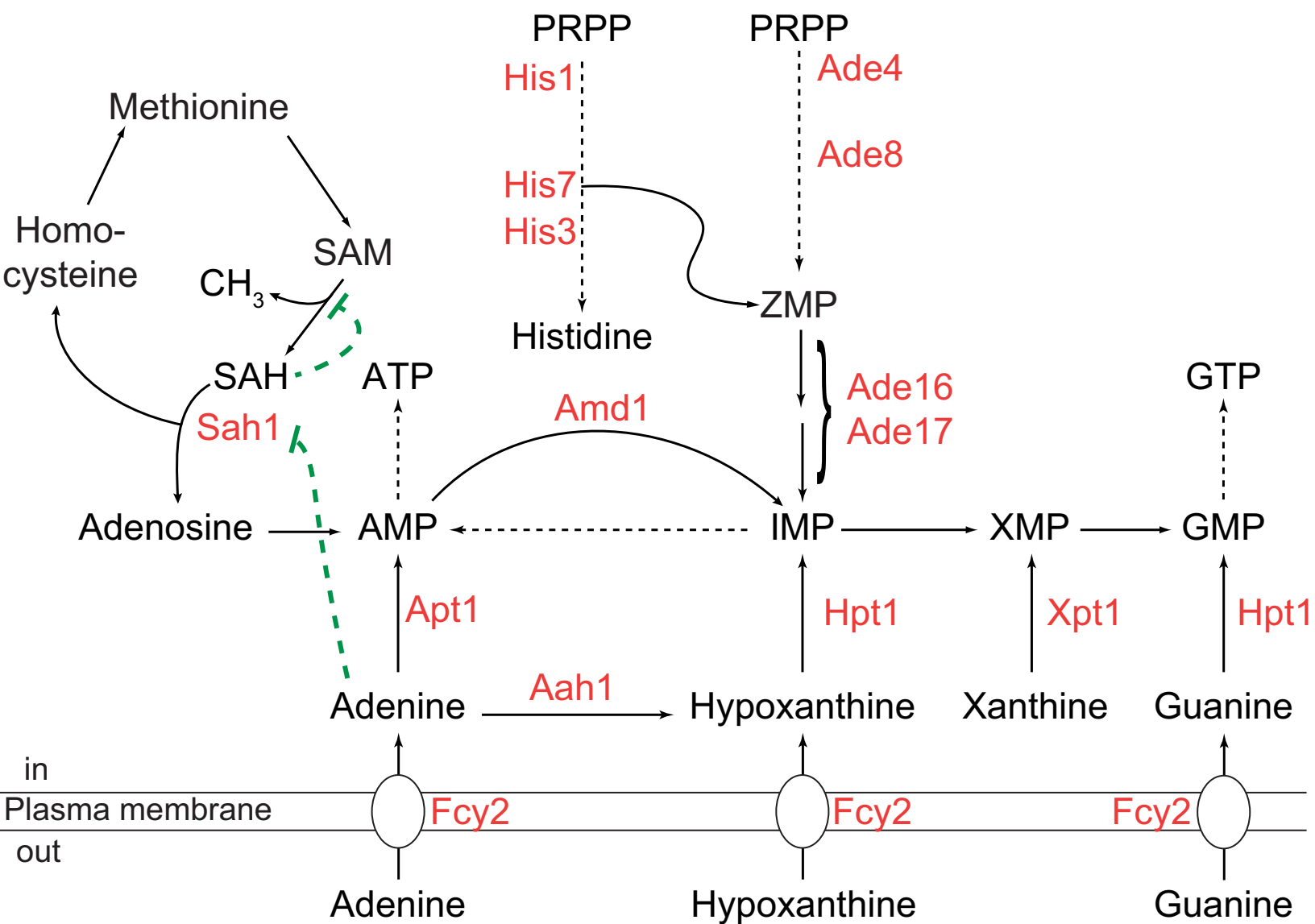
595

596

**Table 2** Plasmids used in this study

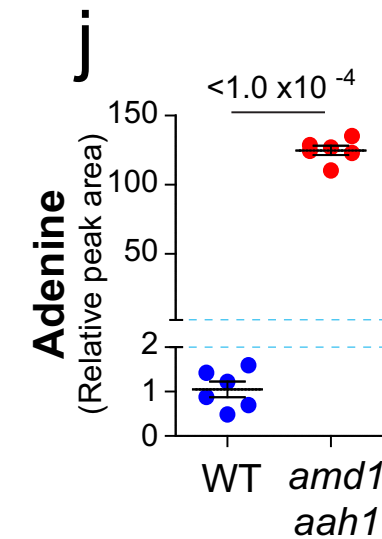
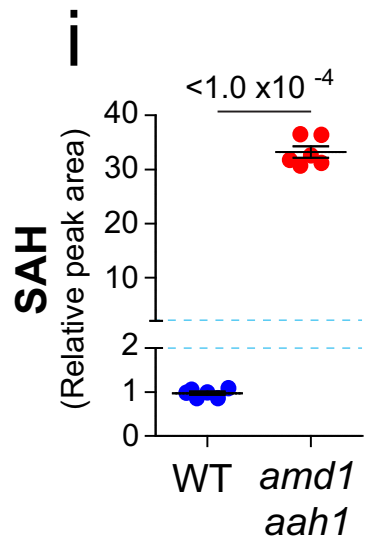
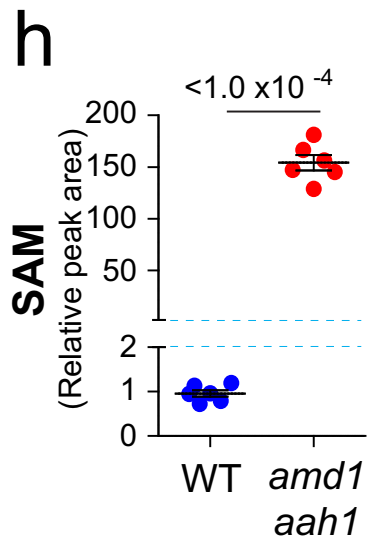
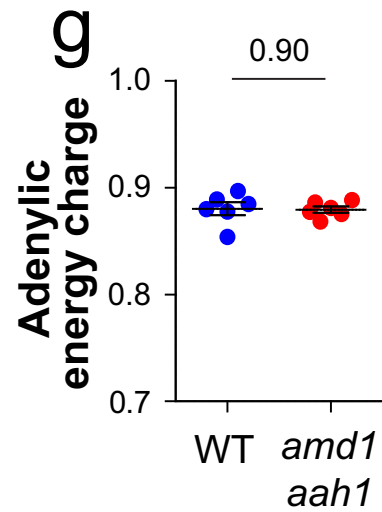
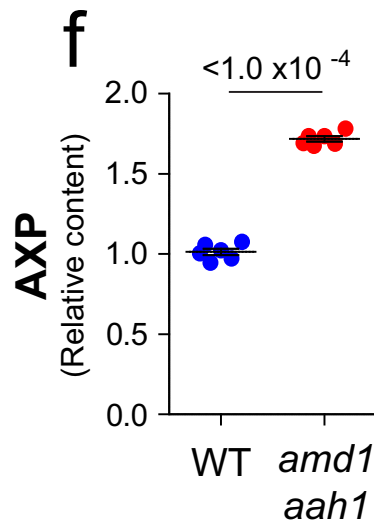
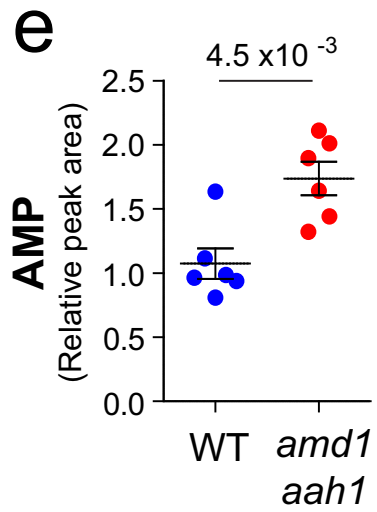
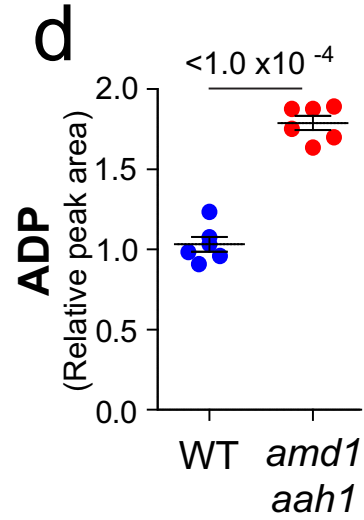
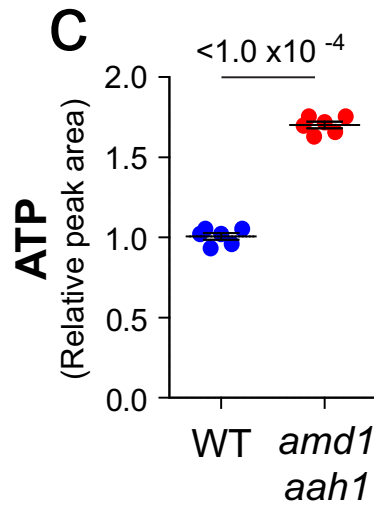
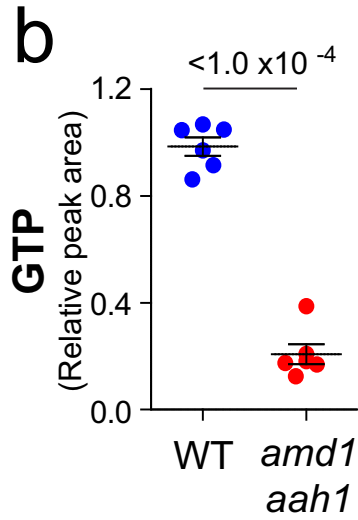
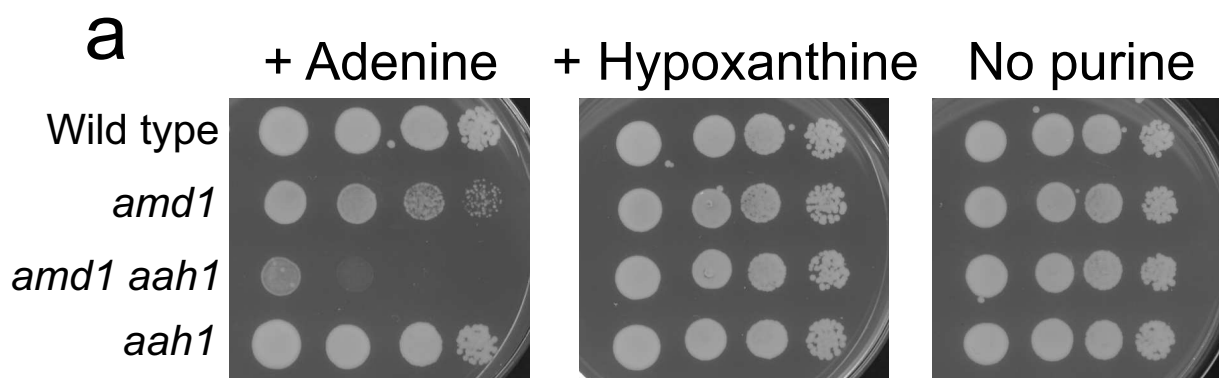
Plasmid	Backbone	Characteristics	References
pCM189	pCM189	<i>CEN ARS URA3 tet-OFF promoter</i>	(Gari et al., 1997)
YCpLac111	YCpLac111	<i>CEN ARS LEU2</i>	(Gietz and Sugino, 1988)
YEplac195	YEplac195	2 $\mu$ m <i>URA3</i>	(Gietz and Sugino, 1988)
pFL44L	pFL44L	2 $\mu$ m <i>URA3</i>	(Bonneaud et al., 1991)
p1933	pCM189	<i>CEN ARS URA3 tet-OFF prom-ADE4</i>	(Rebora et al., 2001)
p2191	YCpLac111	<i>CEN ARS LEU2 HIS3</i>	(Rebora et al., 2005)
P3332	pFL44L	2 $\mu$ m <i>URA3 HIS1</i>	Lab Collection
p5011	YEplac195	2 $\mu$ m <i>URA3 APT1</i>	Lab Collection
p5839	pFL44L	2 $\mu$ m <i>URA3 TAT1</i>	This study
p5840	pFL44L	2 $\mu$ m <i>URA3 PIK1</i>	This study
p5841	pFL44L	2 $\mu$ m <i>URA3 ADE4</i>	This study
p5842	pFL44L	2 $\mu$ m <i>URA3 HIS1</i>	This study
p5847	pFL44L	2 $\mu$ m <i>URA3 RPL35B-RDII-PPH21</i>	This study
p5894	pFL44L	2 $\mu$ m <i>URA3 XPT1</i>	This study
p5896	pFL44L	2 $\mu$ m <i>URA3 ADE4 LIP1 DIN3</i>	This study
p5897	pFL44L	2 $\mu$ m <i>URA3 HYM1</i>	This study
p5898	pFL44L	2 $\mu$ m <i>URA3 ERC1</i>	This study
p5899	pFL44L	2 $\mu$ m <i>URA3 MSN2</i>	This study
p5900	pFL44L	2 $\mu$ m <i>URA3 BAP2</i>	This study
p5901	pFL44L	2 $\mu$ m <i>URA3 AAH1</i>	This study
p5902	pFL44L	2 $\mu$ m <i>URA3 HPT1</i>	This study
P6026	pFL44L	2 $\mu$ m <i>URA3 APT2 DOT1</i>	This study

Figure 1



Saint-Marc *et al*  
Figure 1

Figure 2



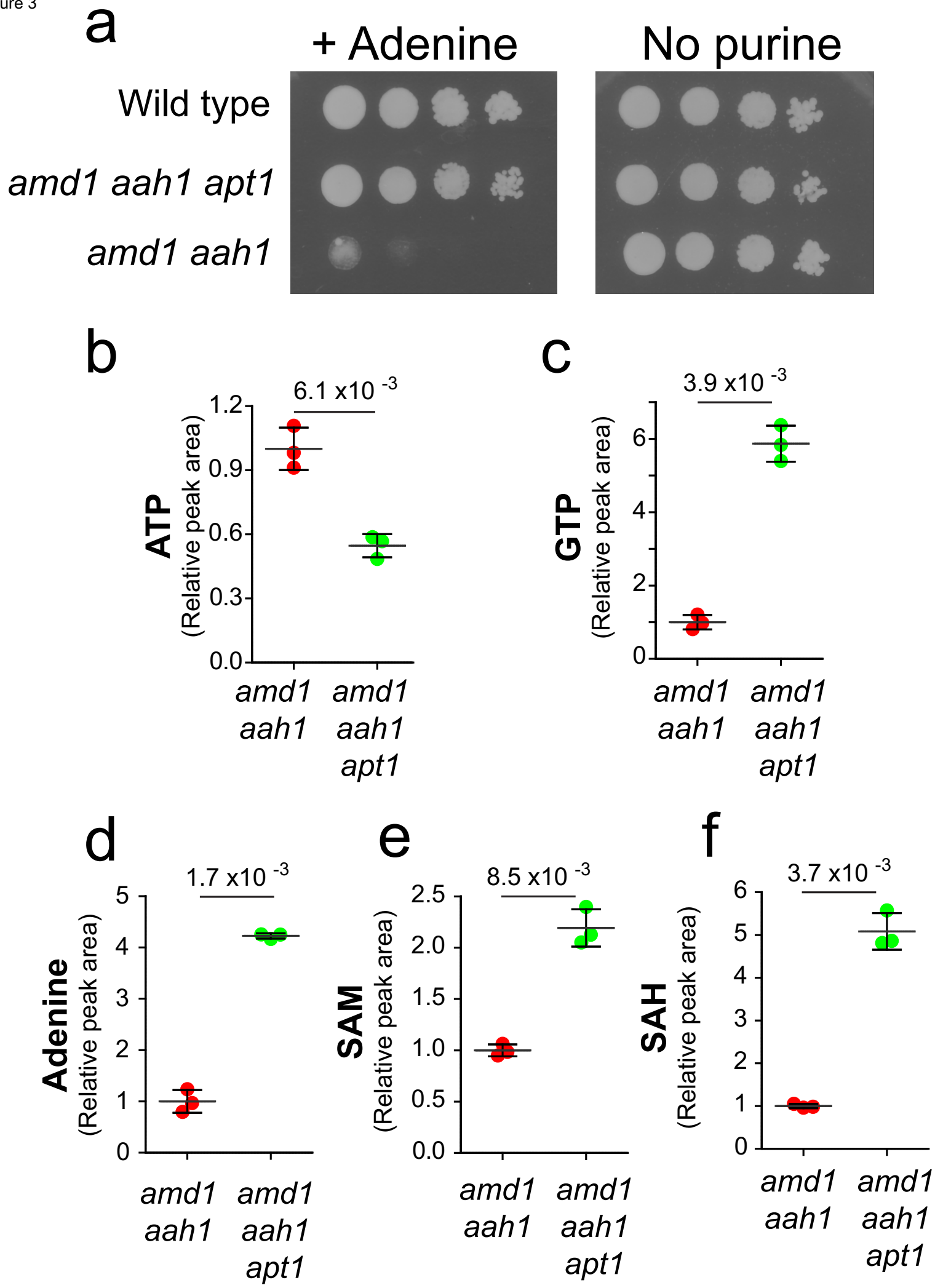


Figure 4

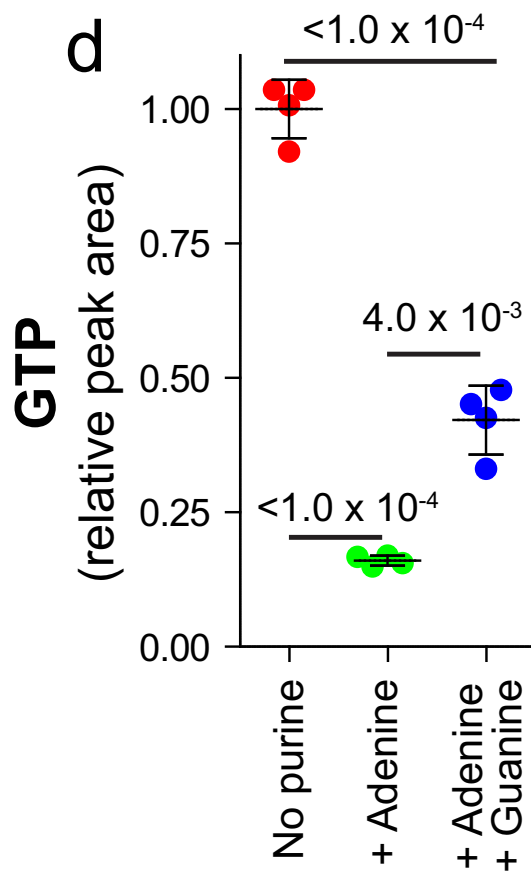
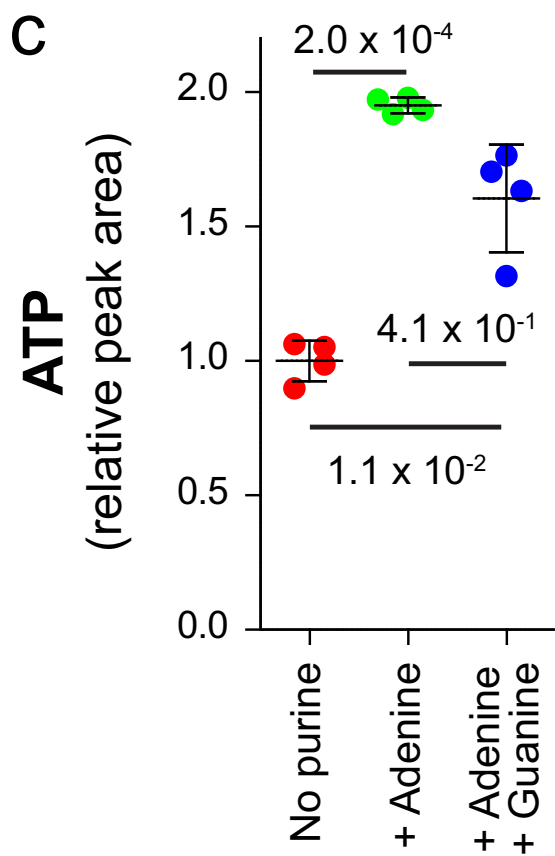
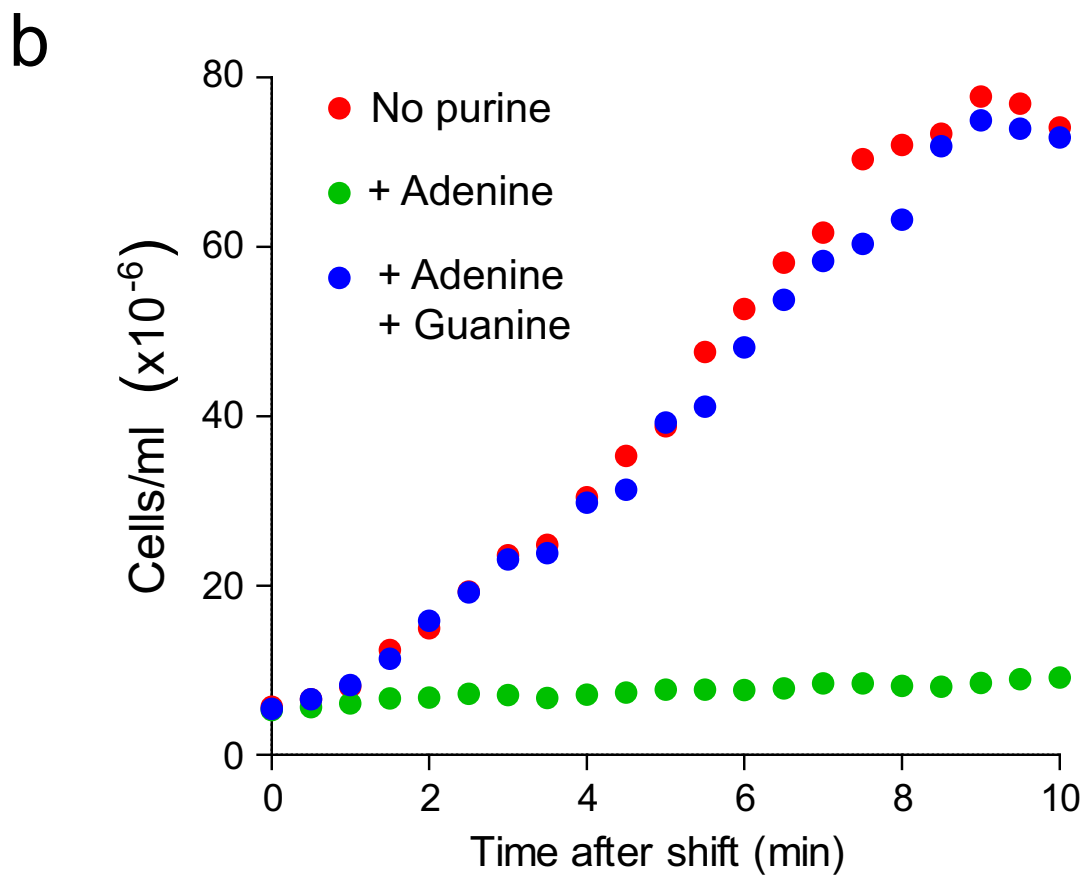
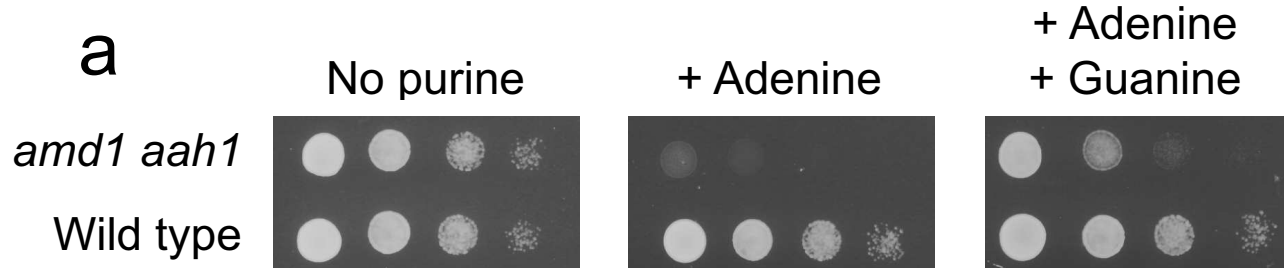


Figure 5

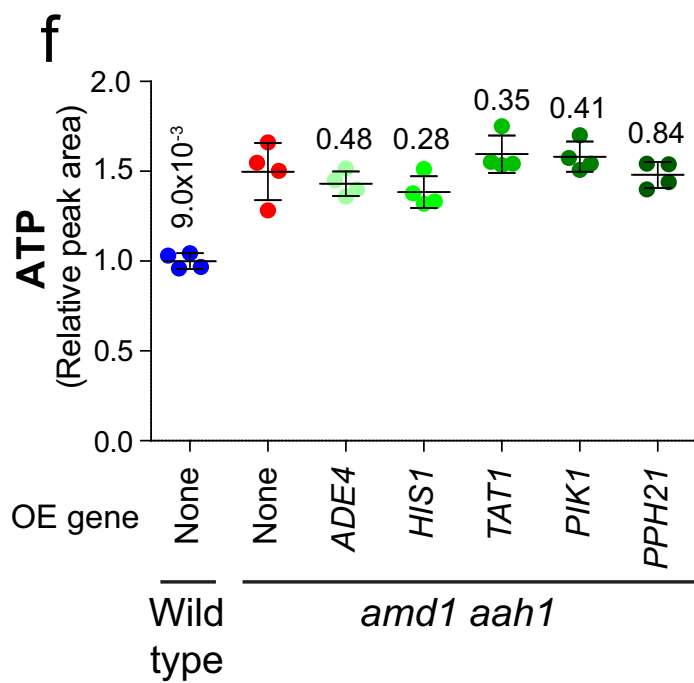
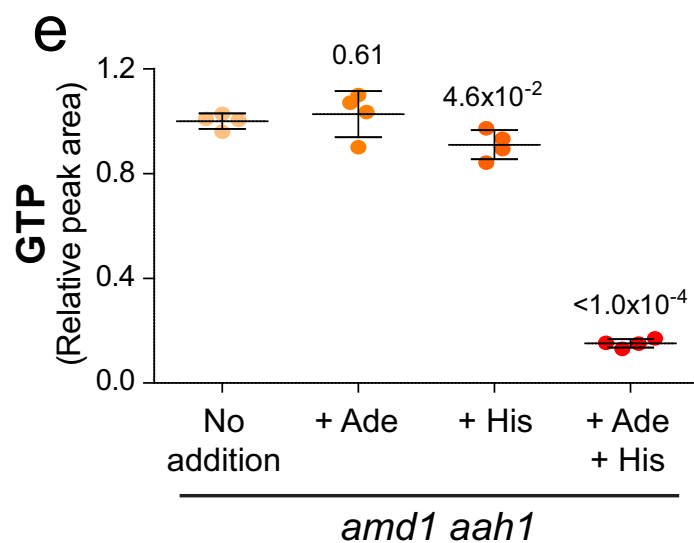
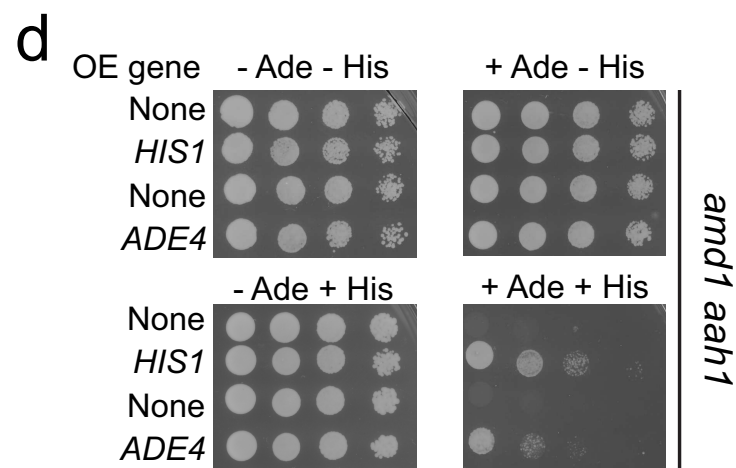
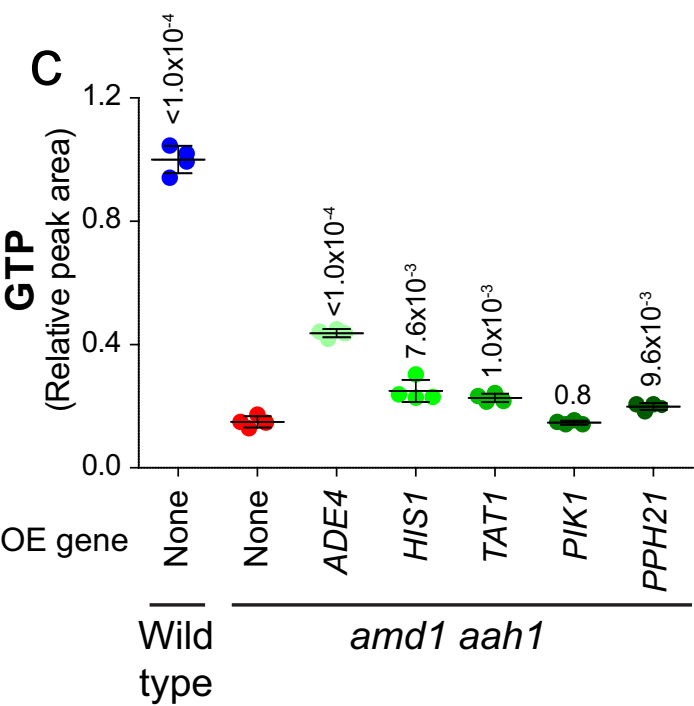
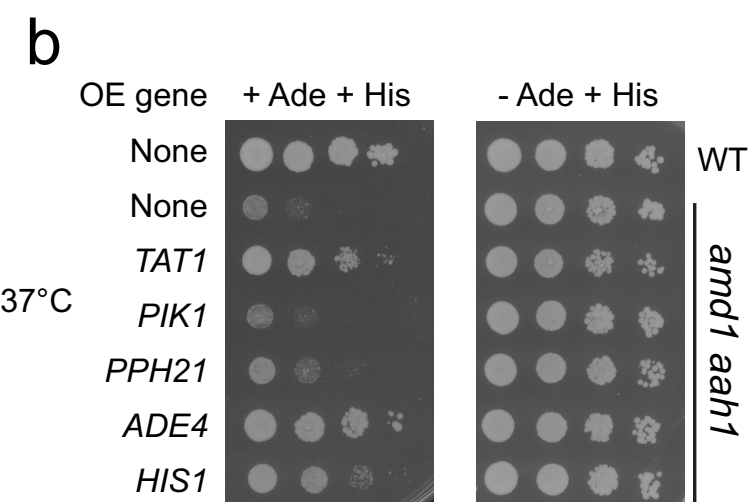
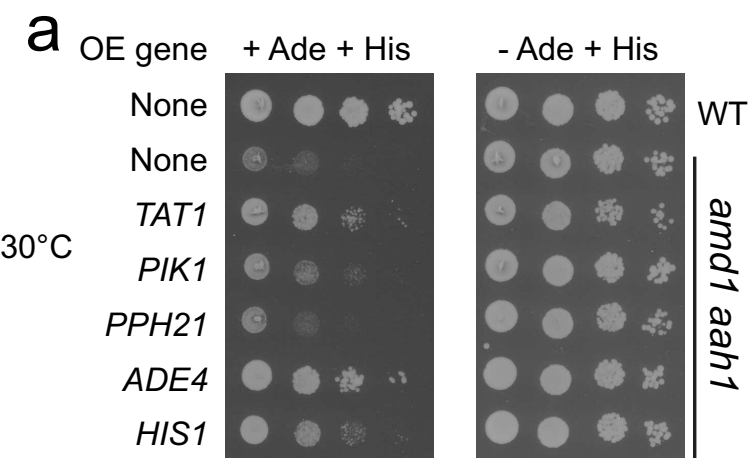


Figure 6

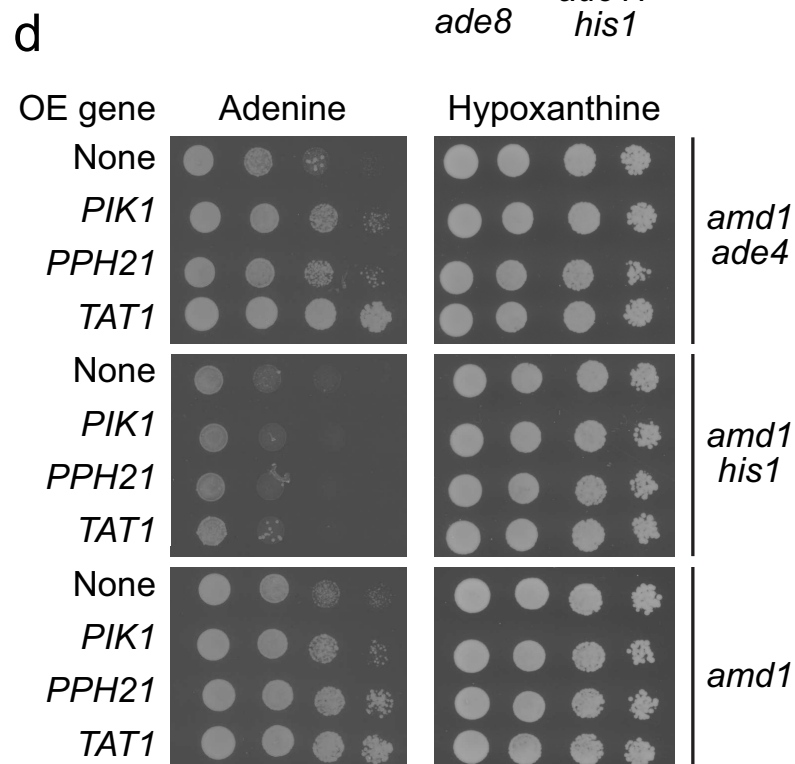
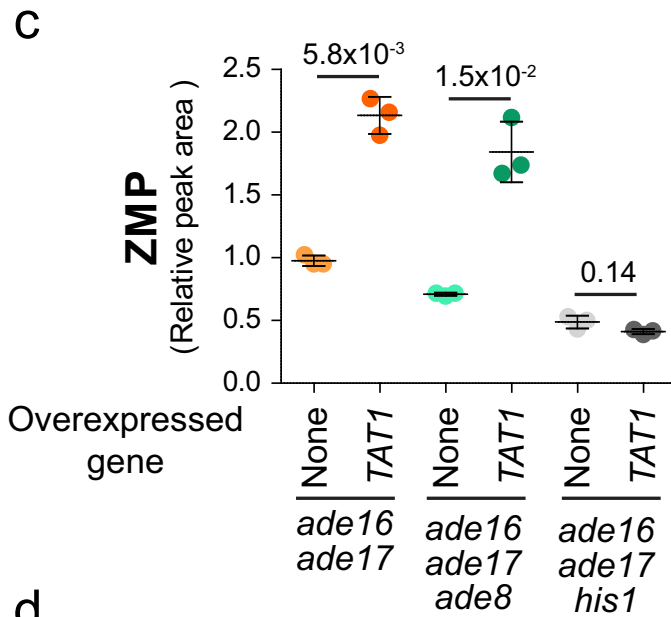
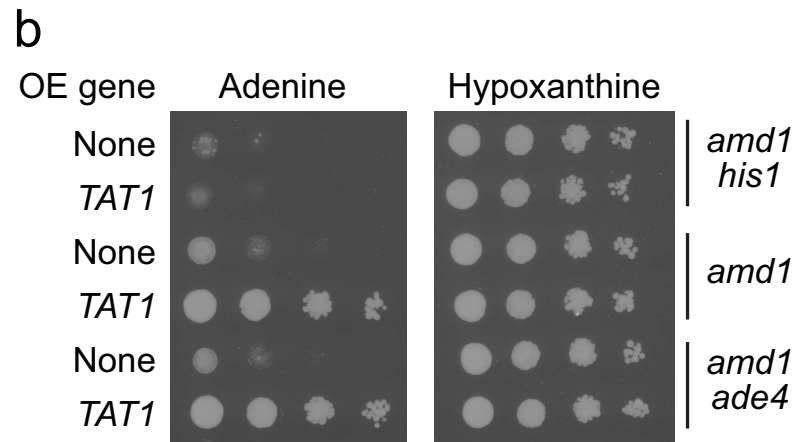
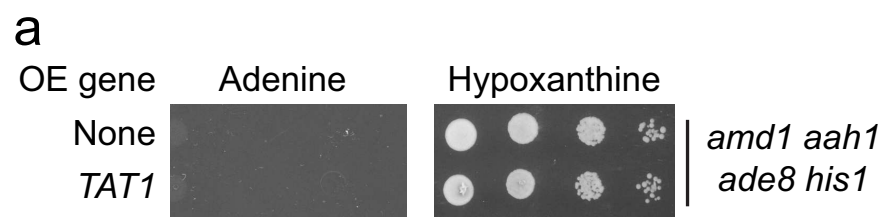
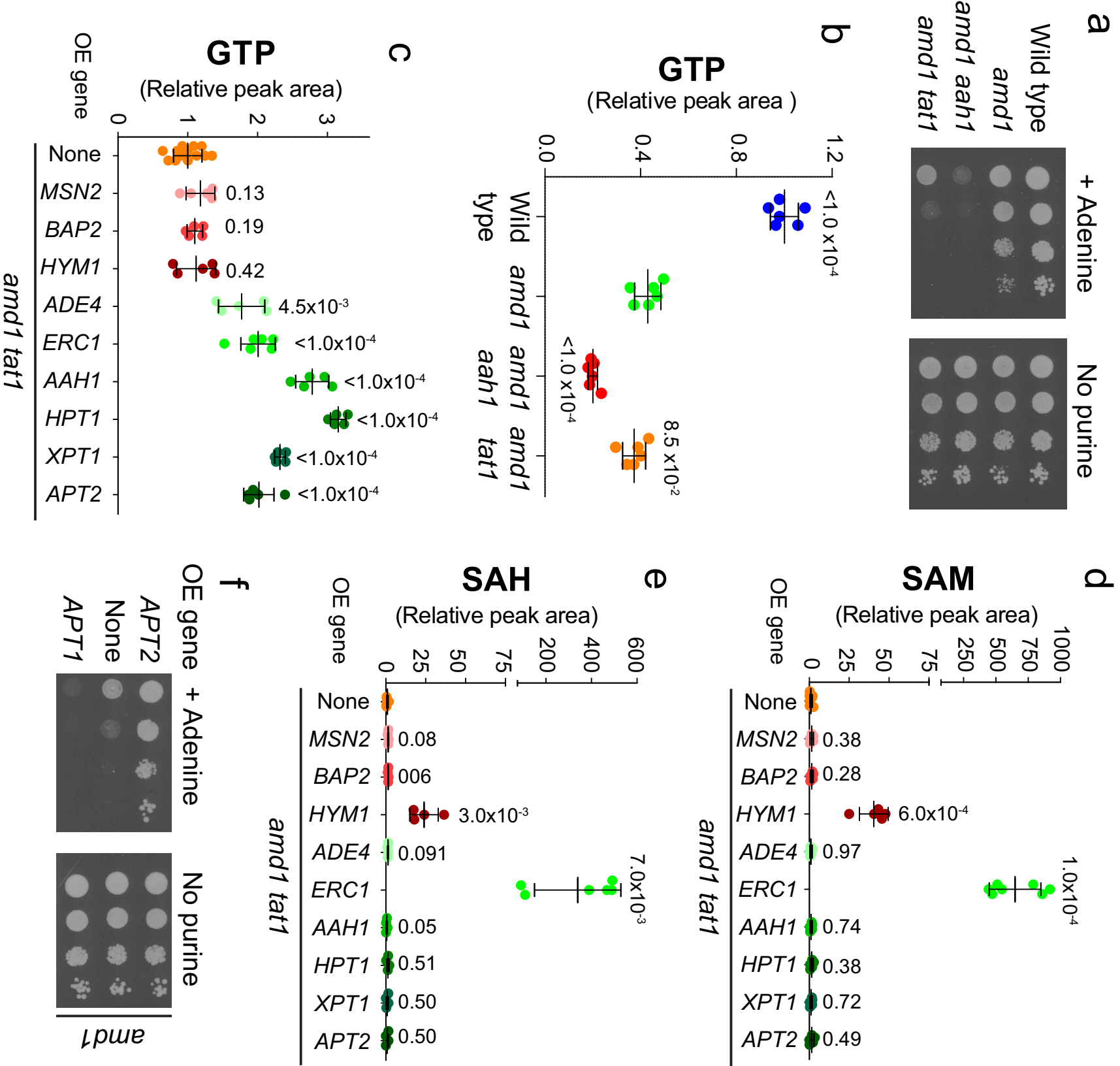
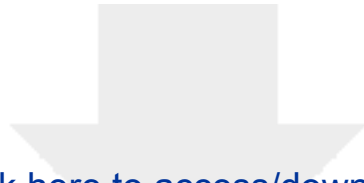


Figure 7





[Click here to access/download](#)

**Supplementary Material**

Saint Marc et al Supplemental data.pdf

